tvst

Article

Assessment of Diabetic Choroidopathy Using Ultra-Widefield Optical Coherence Tomography

Nicolò Nicolini[1,2], Beatrice Tombolini[1,2], Costanza Barresi[1,2], Francesco Pignatelli[3], Rosangela Lattanzio[2], Francesco Bandello[1,2], and Maria Vittoria Cicinelli[1,2]

[1] School of Medicine, Vita-Salute San Raffaele University, Milan, Italy
[2] Department of Ophthalmology, IRCCS San Raffaele Scientific Institute, Milan, Italy
[3] Department of Ophthalmology, SS Annunziata Hospital, Taranto, Italy

Correspondence: Maria Vittoria Cicinelli, Department of Ophthalmology, San Raffaele Vita-Salute University, Via Olgettina, 60, 20132 Milano, Italy.
e-mail: cicinelli.mariavittoria@hsr.it

Received: October 14, 2021
Accepted: March 11, 2022
Published: March 30, 2022

Keywords: diabetic retinopathy; choroidal vascularity index; swept-source optical coherence tomography; ultra-widefield imaging

Citation: Nicolini N, Tombolini B, Barresi C, Pignatelli F, Lattanzio R, Bandello F, Cicinelli MV. Assessment of diabetic choroidopathy using ultra-widefield optical coherence tomography. Transl Vis Sci Technol. 2022;11(3):35, https://doi.org/10.1167/tvst.11.3.35

Purpose: The purpose of this study was to investigate a confocal scanning laser ophthalmoscopy (cSLO) ultra-widefield (UWF) swept-source optical coherence tomography (SS-OCT) in assessment of diabetic choroidopathy and to evaluate the agreement of measurements with a spectral-domain OCT (SD-OCT) instrument.

Methods: We conducted a cross-sectional study of patients with diabetes evaluating the choroidal vascularity index (CVI) in the nasal, temporal, and central macula segments of a UWF SS-OCT scan centered to the fovea. UWF pseudocolored fundus images were used for diabetic retinopathy (DR) severity staging. The CVI values were compared between different degrees of severity of DR and different posterior-pole sectors with linear mixed models. Central macula CVI measurements were repeated on SD-OCT scans; the inter-observer intraclass coefficient (ICC) was calculated between SS-OCT and SD-OCT.

Results: A total of 151 eyes of 85 patients were included. The CVI values decreased from nonproliferative DR to proliferative DR, with high-risk proliferative DR having significantly lower CVI values than moderate to severe nonproliferative DR ($P = 0.03$). The central macula region was the most evidently affected; the nasal sector was the least affected. The agreement between SS-OCT and SD-OCT was moderate (ICC = 0.50).

Conclusions: Diabetic choroidopathy progresses with worsening of DR toward proliferative disease; choroidal depletion is more prominent in the macula. Caution is recommended in comparing CVI values between different devices.

Translational Relevance: Choroidal vascularity informs about the severity of DR and its complications, such as macular edema. The agreement between readers and between instruments may be suboptimal in certain cases.

Introduction

The study of the choroid has drawn increasing scientific attention in the latest years. Normal and pathologic choroidal features have been characterized in healthy and diseased subjects. Post mortem and in vivo studies have pointed toward a progressive choroidal depletion in diabetes.[1,2] Vascular degeneration, aneurysms, neovascularization, choriocapillaris dropout, vessels' narrowing, and increased tortuosity have been described in the choroid of patients with diabetes. All these changes have been collectively addressed as diabetic choroidopathy.[3,4] As most research has focused on the macular region, the extramacular choroidal changes in diabetic eyes have remained largely unexplored.

Due to its high resolution and widespread availability, optical coherence tomography (OCT) has outweighed other imaging modalities, such as color fundus photography or fluorescein angiography, in diagnosing and following patients with diabetes. OCT allows for the quantitative evaluation of the retinal and choroidal thickness, fluid localization, retinal layers' integrity, and segmentation.[5] The recent integration of OCT with ultra-widefield cameras (UWF) has ushered into a new era of ocular imaging, rendering high-definition, expanded field-of-view (FOV) morphologic

snapshots of the retinal and choroidal periphery.[6–8] Parallelly, robust quantitative metrics, such as the choroidal vascularity index (CVI), have been developed to diagnose, classify, and monitor retinal diseases.[9] The macular CVI has been proposed as a novel OCT-based imaging biomarker of diabetic choroidopathy.[10]

The present study investigates the choroidal changes and their topographic distribution in a pool of patients with diabetes using a confocal scanning laser ophthalmoscopy (cSLO) expanded-FOV swept-source OCT (SS-OCT). We tested whether the peripheral CVI values varied as a function of the severity of diabetic retinopathy (DR), as previously demonstrated in the macular region.[10–12] The secondary aim was to assess the inter-rater repeatability of CVI measurements in the macula and the agreement with a conventional spectral-domain OCT (SD-OCT) instrument.

Methods

This is a cross-sectional study of patients with diabetes prospectively enrolled at the Medical Retinal Unit of the Department of Ophthalmology of San Raffaele Scientific Hospital from February 2021 to August 2021. The procedures followed the tenets of the Declaration of Helsinki and obtained the institutional review board approval for noninterventional studies (OCTA_MIMS, v1, 2021).

Patients were included if they were older than 18 years and diagnosed with diabetes mellitus (DM), type 1 or type 2. Patients were excluded if they had a retinal disease other than DR (e.g. age-related macular degeneration, retinal vein occlusion, and uveitis), DR-related complications impeding retinal imaging (e.g. vitreous hemorrhage, retinal detachment, or corneal edema from neovascular glaucoma), history of intraocular surgery within the past 3 months, or uncontrolled glaucoma (i.e. progressive disease despite maximal treatment). Patients with media opacity, such as dense cataract, or posterior-segment evident abnormalities (e.g. myopic staphyloma and coloboma) were also excluded. Additional exclusion criteria included end-stage renal disease, congestive heart failure, and systemic inflammatory diseases, such as sarcoidosis, systemic sclerosis, and vasculitides, because all these conditions could potentially affect the choroidal structure and thickness.

The sample size was arrived at using the paper from Gupta et al. as a reference.[10] In detail, setting the mean ± standard deviation (SD) CVI of group 1 (mild DR) at 66.38 ± 0.31 and the mean of group 2 (proliferative DR [PDR]) at 61.27, we obtained a sample size of 36 with a power of 80% and a risk of alpha error of 0.05. Both eyes of the same patient were included if eligible.

Study Procedures

Demographic and clinical data were collected for each participant; history of previous treatments for DR (such as pars plana vitrectomy [PPV] or panretinal photocoagulation [PRP]) or diabetic macular edema (DME), such as intravitreal injections of anti-vascular endothelial growth factor (VEGF) agents or dexamethasone (DEX) implant, was retrieved from the patients' medical charts. All subjects underwent best-corrected visual acuity (BCVA), slit-lamp biomicroscopy, and dilated fundus examination before imaging.

All patients were imaged with the Optos Silverstone extended-FOV SS-OCT (Optos PLC; Dunfermline, UK).[13] All the examinations were performed by three trained ophthalmology residents (authors B.T., C.B., and N.N.). The SS-OCT scan was executed with a scanning speed of 100,000 A-scans per second and a wavelength-sweeping laser with a central wavelength of 1050 nm. The scan was centered onto the foveal depression or the presumed foveola if obliterated by macular edema; the scan was registered with a central 200 degree single-capture red/green pseudocolored image. Poor-quality scans (signal-to-noise ratio [SNR] <10/10) or images that were peripherally inverted were discarded from the analysis. A subset of patients underwent SD-OCT (Spectralis HRA + OCT; Heidelberg Engineering, Heidelberg, Germany) with an enhanced-depth imaging (EDI) modality within the same visit. SD-OCT scans with SNR below 25 decibels were not used for the analysis.[14]

DR Grading

The pseudocolored fundus images were stereographically projected by the Optos software and used for DR severity grading. The grading was done by a fellowship-trained retina specialist (author M.V.C.). DR stages were derived from a simplified version of the Early Treatment Diabetic Retinopathy Study (ETDRS) Diabetic Retinopathy Severity Scale (DRSS) and included: no retinopathy (level 10), mild nonproliferative DR (NPDR; levels 20–35), moderate to severe NPDR (levels 43–53), mild PDR (level 61), and moderate to high-risk PDR (levels 65—75; see Supplementary Table S1).[15]

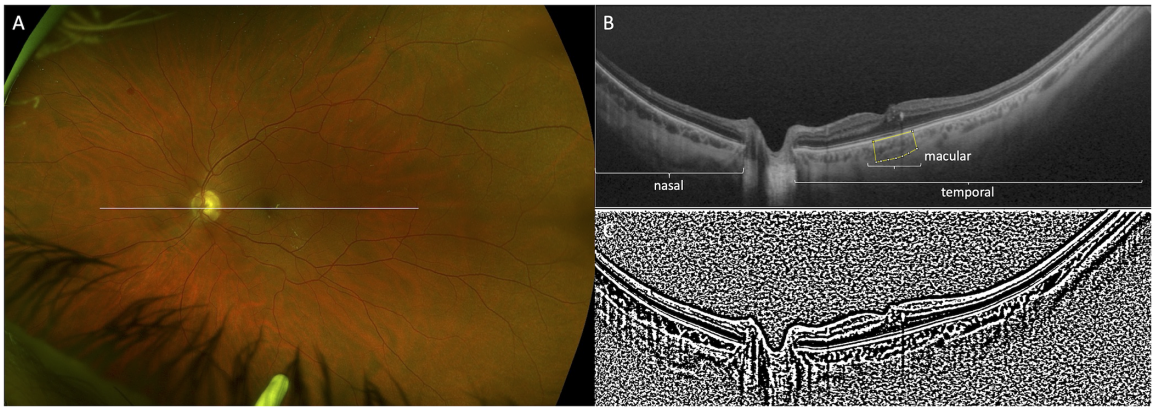

Figure 1. Measurement of the choroidal vascularity index (CVI) on extended-field of view swept-source optical coherence tomography (SS-OCT). (**A**) Pseudocolored fundus image of a patient with nonproliferative diabetic retinopathy, with hard exudates in the macula and a few hemorrhages in the periphery. (**B**) SS-OCT scan passing through the fovea, showing macular microaneurysm and intraretinal hyperreflective spots corresponding to the hard exudates. The areas corresponding to the central macula, the temporal, and the nasal choroidal vascularity index are indicated. The yellow polygon shows the actual area in which the central macula choroidal vascularity index was calculated. The total choroidal vascularity index was the sum of the nasal and the temporal areas. (**C**) The SS-OCT scan was digitally binarized; within the choroid, the dark pixels represent the luminal choroidal areas, and the white pixels correspond to the stromal choroidal areas.

CVI Measurements

The CVI measurements on extended-FOV SS-OCT were performed by one single reader (author N.N.), who was masked to the DR grading (Fig. 1). All the OCT scans were anonymized, exported as JPEG, and analyzed on the open software ImageJ (version 1.46r).[16] All the OCT scans were processed with a size of 2552 × 828 pixels. A scaling factor was then set, considering a horizontal length of 23 mm.

The CVI was calculated as previously reported.[17] In brief, the horizontal OCT scans were binarized using the Niblack threshold. The total choroidal area (TCA; mm^2) was calculated as the polygon having as upper boundary the retinal pigment epithelium and as the lower boundary the sclero-choroidal junction. The dark pixels corresponding to the choroidal vascular spaces were highlighted and considered as the luminal choroidal area (LCA; mm^2). The CVI was the ratio between the LCA and the TCA and expressed as a percentage.

The CVI measurements were repeated in three separate segments: the nasal segment, from the nasal edge of the optic nerve to the end of the visualized nasal choroid; the temporal segment, from the temporal edge of the optic nerve to the end of the visualized temporal choroid; and the central macula segment, corresponding to a 1500-μm wide area centered on the fovea. Finally, the nasal LCA and the temporal LCA were summed together and divided by the sum of the nasal TCA and the temporal TCA, to obtain the total CVI. Therefore, each patient had a total CVI, a nasal CVI, a temporal CVI, and a central macula CVI. The subfoveal choroidal thickness was manually measured with the Optos Silverstone caliber.

To assess the repeatability and the agreement between extended-FOV SS-OCT and conventional SD-OCT, the central macula CVI values were also calculated on SD-OCT scans obtained in 87 eyes of 56 patients. The same 1500-μm wide area centered on the fovea was used as the region of interest. The central macula OCT scans were divided into two subgroups: one subset ($N = 56$ eyes) was measured by reader 1 (author N.N.) and reader 2 (author B.T.); the other subset ($N = 31$ eyes) was measured by reader 1 (N.N.) and reader 3 (author C.B.). The two pairs of readers independently performed the measurements on both extended-FOV SS-OCT and conventional SD-OCT.

Statistical Analysis

All the statistical calculations were conducted with the open-source programming language R (version 1.2.5033).[18] The cutoff point for statistical significance was $P < 0.05$. Descriptive statistics of continuous variables were reported as mean ± SD; qualitative variables were reported as frequency and percentage proportions.

For the primary outcome, we compared the CVI values between different degrees of DR severity and between different posterior-pole sectors. We used a linear mixed model where the CVI was the main outcome variable, the DR stage (no DR, mild NPDR, moderate to severe NPDR, mild PDR, and moderate

to high-risk PDR) and the sector (i.e. central macula, nasal, and temporal) were the main explanatory variables, and the patients' and eyes' identification numbers (IDs) were nested random factors, to correct for both eyes included for the same patients and multiple sectors acquired in the same eye, respectively. Pairwise groups were compared with Tukey's adjustments. Associations between demographic and clinical factors and the central macula and the total CVI were sought with linear mixed models. Beta (β) regression estimates and 95% confidence interval (CI) are provided, after inspection of the models' residuals. As a sensitivity analysis, the calculations were repeated in the subset of patients that had never received any treatment for DR or DME.

The secondary outcome was to assess how the repeatability and the agreement of extended-FOV SS-OCT and SD-OCT in measuring the central macula CVI. Pairwise agreement among the three readers was calculated with the interobserver intraclass coefficient (ICC). A two-way fixed-effects model (i.e. the selected raters were fixed and were the only raters of interest), single-rater (i.e. the agreement was measured on the actual measurements instead of their average), and absolute agreement (i.e. the systematic differences between raters were relevant) was used.[19] The intra-rater agreement (i.e. the degree of agreement among repeated CVI measures performed by the same rater), was measured in a similar manner. The ICC value was considered poor if below 0.50, moderate if between 0.50 and 0.75, good if between 0.75 and 0.90, and excellent if above 0.90. The agreement between extended-FOV SS-OCT and SD-OCT was assessed with the ICC and graphically inspected with Bland-Altman (BA) statistics, after confirming the normality of the differences' distribution. The mean CVI values between the two sets of readings were used for plotting the ICC and the BA graph. The limits of agreement (LOA) were set at 1.96 SDs.[20] The percentage difference (PD%) between SD-OCT and extended-FOV SS-OCT was calculated as the absolute value of the difference between two measurements divided by the average of the same values and multiplied by 100. Factors influencing the PD% were explored using linear or quadratic regression models, according to data distribution.

Results

A total of 171 eyes of 95 patients with diabetes were imaged. Twenty eyes were excluded because of poor quality OCT scans or concomitant retinal pathology.

Table 1. Demographic and Clinical Characteristics of the Study Cohort

Patients' characteristics (n = 85)	
Age (years)	63 (IQR = 53 to 70)
Gender:	
Males	48 (57%)
Females	37 (43%)
DM type:	
Type 1	33 (39%)
Type 2	52 (61%)
Eyes' characteristics (n = 151)	
Refraction (diopters)	0.50 (IQR = −0.75 to 1.50)
BCVA (LogMAR)	0.05 (IQR = 0 to 0.15)
DME	61 (40%)
Previous treatments:	
Any anti-VEGF	40 (26%)
• Number of anti-VEGF	5 (IQR = 3 to 8)
Any DEX	24 (16%)
• Number of DEX	1 (IQR = 1 to 4)
Focal laser	26 (17%)
PRP	38 (25%)
PPV	9 (6%)

BCVA, best-corrected visual acuity; DEX, dexamethasone; DM, diabetes mellitus; DME, diabetic macular edema; IQR, interquartile range; PPV, pars plana vitrectomy; PRP, panretinal photocoagulation; VEGF, vascular endothelial growth factor.

Therefore, 151 eyes of 85 patients were included in the statistical analyses. There was a slight prevalence of men (48 men, 57%). Patients' age ranged between 19 and 83 years old, with a mean age of 61 ± 14 years. Table 1 summarizes the main clinic characteristics of patients and eyes. Figure 2 and Supplementary Figure S1 shows the DR severity stage distribution; patients' age was similar between the groups. Of the entire cohort, 74 eyes (49%) had received previous treatments for DR or DME, whereas 77 eyes (51%) were naïve.

Analysis of CVI Between Sectors

There was a topographic distribution of the CVI, being the highest in the central macula and then reducing toward the periphery. The CVI values in the nasal and temporal sectors were similar ($P = 0.1$) and correlated ($r^2 = 0.24$, 95% CI = 0.08 to 0.40, $P = 0.005$).

The CVI decreased from NPDR to more severe categories in all sectors (Table 2, Fig. 3A). Multiple comparisons revealed a substantial difference between moderate to severe NPDR and high-risk

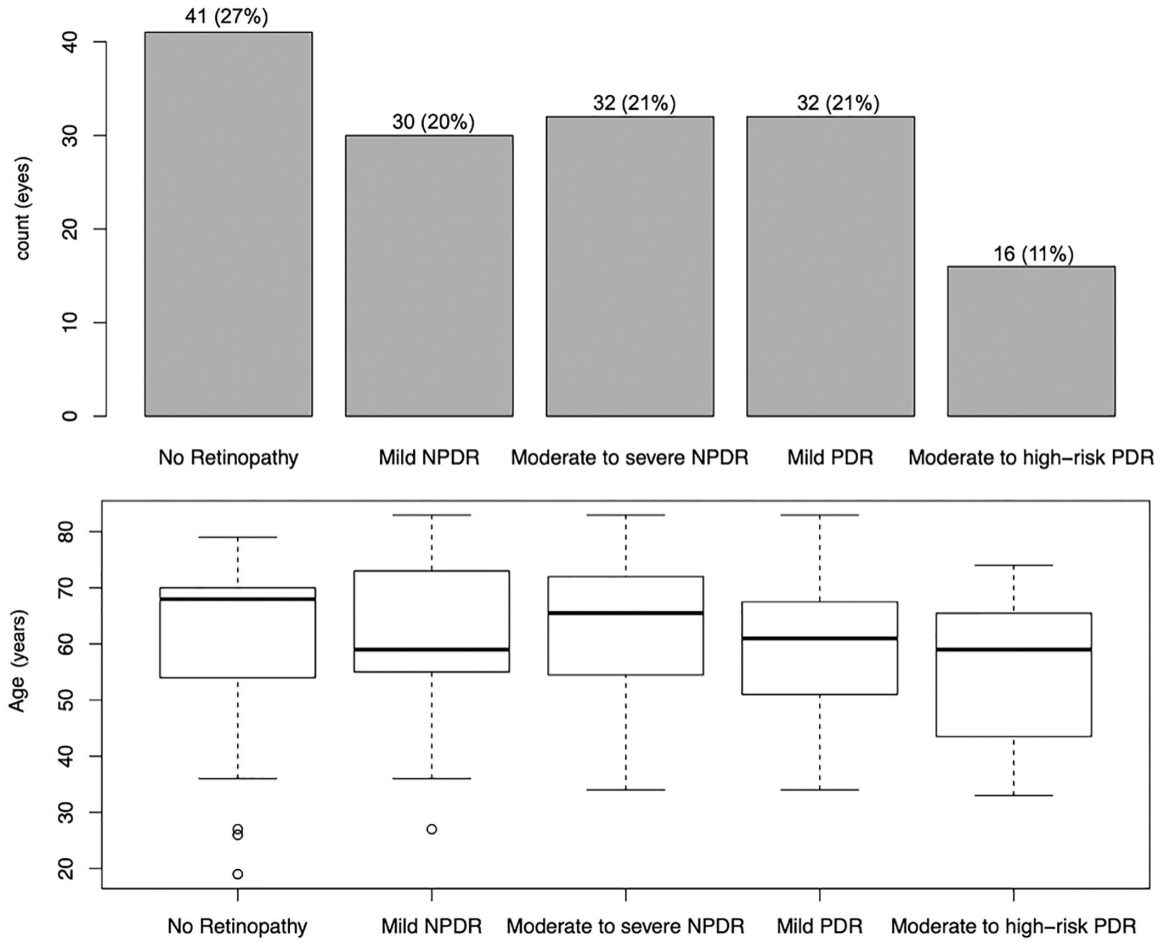

Figure 2. Sample size stratified according to the diabetic retinopathy (DR) severity stage. Upper quadrant: Bar plots indicating the sample size, according to no DR, nonproliferative DR (NPDR), and proliferative DR (PDR). Lower quadrant: Boxplots of age, showing a non-significant difference in age between DR categories.

Table 2. Choroidal Vascularity Index (CVI) Values Stratified According to the Severity of Diabetic Retinopathy (DR)

	Total CVI (%)	Nasal CVI (%)	Temporal CVI (%)	Central Macular CVI (%)
No retinopathy ($n = 41$)	65.6 ± 4.1	65.8 ± 6.2	65.1 ± 3.9	68.8 ± 4.2
Mild NPDR ($n = 30$)	65.1 ± 4.4	64.2 ± 4.5	64.9 ± 3.6	68 ± 4.4
Moderate to severe NPDR ($n = 32$)	67 ± 3.8	66.7 ± 6.7	67.6 ± 4.1	68.3 ± 5.1
Mild PDR ($n = 32$)	65.2 ± 2.8	63 ± 6.6	65.9 ± 2.9	67.4 ± 4.8
Moderate to high-risk PDR ($n = 16$)	64.5 ± 3.2	63.6 ± 4.9	64.6 ± 3.1	66.5 ± 1.5
All eyes ($n = 151$)	65.6 ± 3.8	64.9 ± 6.1	65.7 ± 3.7	66.1 ± 4.4

NPDR, nonproliferative diabetic retinopathy; PDR, proliferative diabetic retinopathy.

PDR ($P = 0.03$). By analyzing the choroidal sectors separately, the most evident decline in CVI values with DR progression from NPDR to PDR was found in the central macula region ($P = 0.03$), followed by the temporal ($P = 0.05$) quadrant. The nasal was apparently not affected ($P = 0.9$). A similar distribution was observed in naïve patients (Supplementary Fig. S2).

Factors Affecting the CVI on Expanded-FOV SS-OCT

None of the investigated demographic and clinical factors was associated with the total CVI. The CVI values were similar between patients with type 1 and type 2 diabetes, even after including the duration of diabetic disease as the interaction term in the statistical

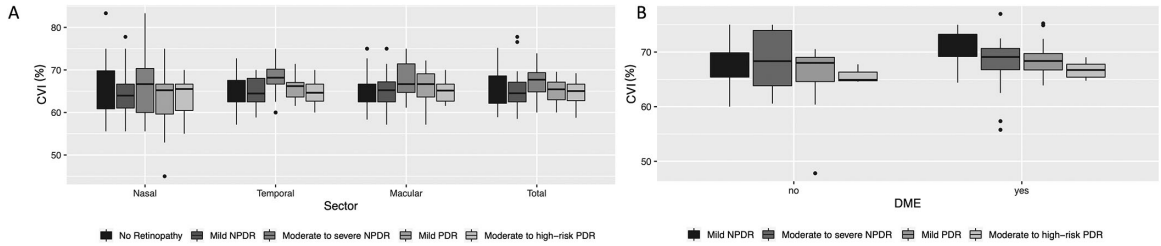

Figure 3. Choroidal vascularity index (CVI) distribution according to diabetic retinopathy (DR) severity stage and ocular sector. (**A**) The CVI progressively increased from mild NPDR to moderate-to-severe NPDR, and then decreased toward high-risk PDR in all sectors. (**B**) CVI values stratified by the presence of diabetic macular edema (DME). Eyes with DME had significantly higher CVI values than eyes without DME.

Table 3. Inter-Rater and the Inter-Instrument Agreement

Reader 1 vs. Reader 2	
Extended-FOV SS-OCT (n=56 eyes)	ICC = 0.25, 95% CI 0.03 to 0.44
SD-OCT (n = 56 eyes)	ICC= 0.28, 95% CI = 0.12 to 0.44
Reader 1 vs. Reader 3	
Extended-FOV SS-OCT (n = 31 eyes)	ICC = 0.55, 95% CI = 0.42 to 0.66
SD-OCT (n = 31 eyes)	ICC = 0.50, 95% CI = 0.35 to 0.62
Extended-FOV SS-OCT versus SD-OCT	
(n = 87 eyes)	ICC = 0.50, 95% CI = 0.35 to 0.62

CI, confidence interval; FOV, field of view; ICC, interobserver intraclass coefficient; SD-OCT, spectral-domain optical coherence tomography; SS-OCT, swept-source optical coherence tomography.

model ($P = 0.7$ for the central macula CVI and $P = 0.4$ for the total CVI). A history of PRP ($P = 0.4$) or PPV ($P = 0.6$) did not affect the global choroidal vascularity (see Supplementary Table S2). The central macula CVI was significantly higher in patients with DME ($\beta = 7.92\%$, 95% CI = 2.36 to 13.49, $P = 0.003$), but it followed the same negative trend with worsening of DR (Fig. 3B). When only naïve patients were analyzed, the association between the central macula CVI and the presence of DME was not confirmed (Supplementary Table S3); however, only 5 of the 77 naïve eyes had DME, and the analysis was underpowered.

Agreement in Central Macula CVI Between Raters and Between Imaging Modalities

The intra-rater agreement was good (ICC = 0.88 for reader 1, and ICC = 0.83 for readers 2 and 3).

The inter-rater agreement in calculating the central macula CVI was poor to moderate for both the extended-FOV SS-OCT (ICC = 0.25 for reader 1 and reader 2 and ICC = 0.55 for reader 1 and reader 3) and the SD-OCT (ICC = 0.28 for reader 1 and reader 2 and ICC = 0.50 for reader 1 and reader 3; Table 3).

The inter-instrument agreement was moderate (ICC = 0.50). The Bland-Altman analysis showed a nearly zero bias (Fig. 4A), with LOA ranging from -10.2% to 10.3%. Three values fell outside the LOA. The variance was constant, and the differences were normally distributed (Fig. 4B). The mean PD% was 6 ± 5.1% (range= 0.10–27%). Extreme values of CVI on either SD-OCT ($P < 0.001$) or extended-FOV SS-OCT ($P < 0.001$) were associated with higher PD% between the two devices (Figs. 4C, 4D). The DR severity ($P = 0.9$) and the presence of DME ($P = 0.6$) were not associated with the PD%.

Discussion

In this study, we used extended-FOV SS-OCT to investigate diabetic choroidopathy in eyes with different stages of DR. We found that the choroidal vascularity reduced with advanced stages of DR; choroidal depletion was more prominent in the central macula region and less marked in the mid-peripheral sectors. The presence of DME significantly affected the central macula CVI but not the global measurements. There was a moderate agreement between extended-FOV SS-OCT and SD-OCT, but a higher discrepancy was found with extreme CVI values.

Diabetic choroidopathy has been known long before the introduction of noninvasive imaging.[21] Structural

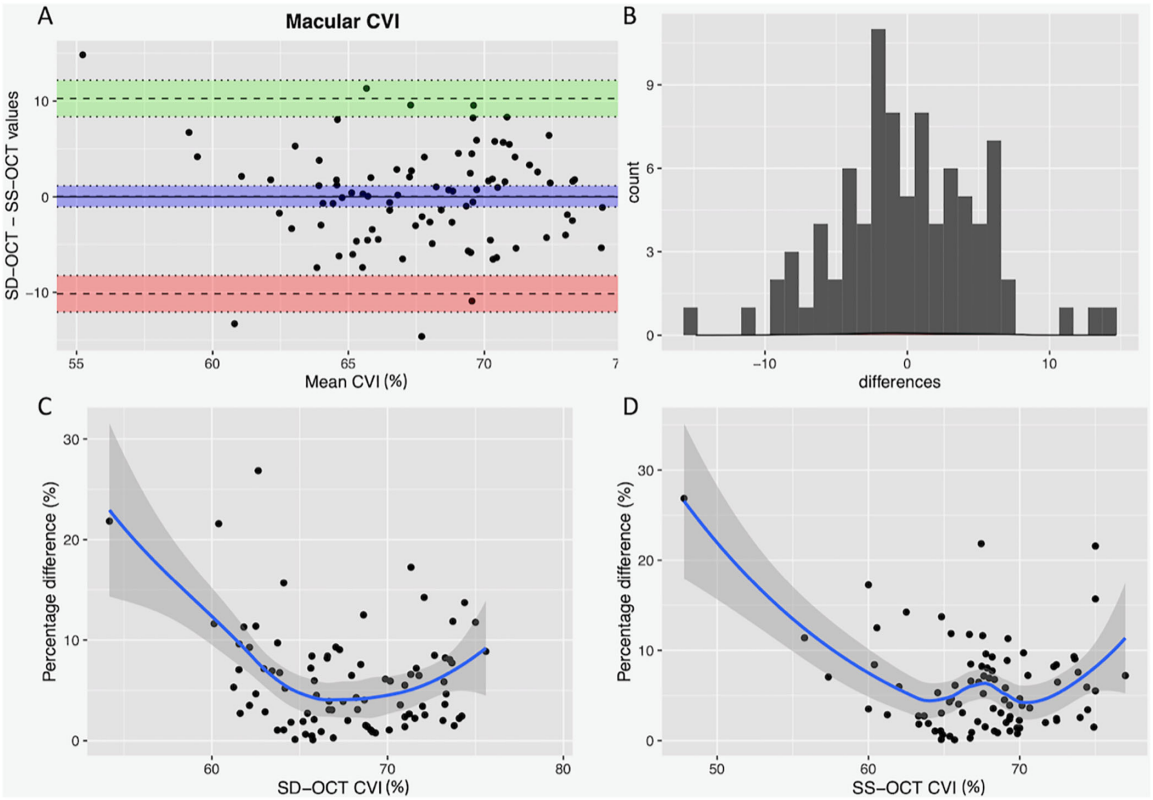

Figure 4. Inter-instrument agreement of central macula choroidal vascularity index (CVI) as measured with swept-source optical coherence tomography (SS-OCT) and spectral-domain optical coherence tomography (SD-OCT). (**A**) The Bland-Altman plot showed almost null bias with wide limits of agreement, ranging from -10.2% to 10.3%. (**B**) CVI differences between the two instruments followed a nearly normal distribution. (**C, D**) CVI measurement differences between the two devices varied as a function of the CVI values and tended to increase with extreme observations of either SD-OCT **C** or SS-OCT **D**.

OCT allowed the study of the choroid in vivo and confirmed choroidal hypoperfusion in patients with DR.[1,10–12] Nevertheless, only a few studies stratified patients with DR according to the DRSS classification.[10,11] Kim et al. studied the macular CVI across five severity groups, namely healthy subjects, no DR, mild/moderate NPDR, severe NPDR, and PDR, in patients with type 2 diabetes. They found that patients with diabetes had lower CVI values than controls, with a significant reduction from NPDR to PDR.[11] We replicated Kim's study using extended-FOV SS-OCT to explore the contribution of mid-peripheral choroidal sectors in the characterization of DR severity. We observed a similar progressive decrease in CVI values from mild to severe DR. The choroidal vascularity peaked in patients with moderate to severe NPDR, and then steeply decreased in proliferative disease. A similar pattern was observed in naïve patients, especially in the central macula. Therefore, we assume lower CVI values in PDR may be due to actual diabetes-induced choroidal depletion or vascular shrinkage, rather than a history of previous treatments.

A topographic variation in the choroidal structure of healthy subjects has been found using extended-FOV OCT[22]; differences between ocular sectors have been interpreted as an uneven distribution of the luminal and the stromal components across the globe. In our study, the central macula had the highest CVI values, and the nasal quadrants had the lowest CVI values, regardless of the stage of DR. The macula receives the highest blood flow from the systemic circulation, thanks to the short posterior ciliary arteries that pierce the sclera just behind the posterior pole.[23] On the other hand, the nasal choroid progressively thins approaching the optic disc, and eventually disappears in the peripapillary region. The nasal CVI also had the highest intragroup disparity (expressed as wider values of SD). As a result, the central macula CVI turned out to be a more informative biomarker of diabetic choroidopathy compared to the peripheral sectors.

Different authors analyzed the clinical associations of diabetic choroidopathy. We found no significant correlations between the total CVI values measured on extended-FOV SS-OCT and age, gender, disease duration, or HbA1c. We tested if the type of diabetes

affected the CVI values. Being affected by type 2 diabetes was associated with overall lower values of CVI, but the difference between type 2 diabetes and type 1 diabetes in CVI values was not significant, accounting for the overall duration of diabetes. The presence of DME was associated with higher CVI values in the central macula but did not affect the global choroidal metrics. Similar to Kim et al.,[11] we found no association between PRP and the CVI, discarding the hypothesis that PRP decreases the choroidal blood flow by lowering the local production of VEGF. We also explored if a history of PPV and history and the number of previous intravitreal injections affected the choroidal structure. Temporary changes in the CVI have been detected in eyes undergoing vitreoretinal surgery[24]; as none of the included eyes had PPV within the previous 3 months, we found no difference in the CVI between vitrectomized and nonvitrectomized eyes. A reduction in both choroidal thickness and CVI[25] has been described in eyes undergoing intravitreal anti-VEGF for age-related macular degeneration. We did not find such a relationship in our cohort of diabetic subjects.

Previously proposed methods based on patients' steering,[26] off-the-shelf devices,[27,28] or manual digital montages,[29] were inadequate for peripheral OCT acquisition due to optical distortion, poor definition, and narrow depth penetration. Advantages of SS-OCT over SD-OCT include deeper signal penetration and faster scan acquisition, allowing better confidence in computing quantitative choroidal measurements. However, only a few studies have assessed the repeatability of SS-OCT measurements. A recent survey from Breher et al. estimated that the intra-session and inter-session repeatability of CVI measurements ranged between 3.90% and 5.50%.[30] We found a moderate inter-rater agreement in calculating the central macula CVI; choroidal measurements in diabetic eyes performed worse compared to a validation study on healthy eyes.[31] Therefore, until automatized methods for CVI calculation are made available, we encourage critical interpretation of CVI measurements, at least in diseased eyes. Extended-FOV SS-OCT and SD-OCT devices had a moderate ICC, slightly lower than reported in healthy subjects (ICC = 0.78).[32] The highest discrepancy between the two instruments was found when the left and the right tails of the CVI distribution were compared. In these cases, interchangeable use of SS-OCT and SD-OCT CVI values is discouraged.

Limitations of this study include the absence of a control group of nondiabetic subjects and the cross-sectional design of data collection. We could not assess if diabetic choroidopathy precedes DR, by assessing the CVI values in nondiabetic subjects. On the other hand, we could not longitudinally assess the rate of CVI decline with DR worsening. We did not assess retinal perfusion with dye angiography or OCT angiography; thus, we were not able to correlate retinal ischemia with diabetic choroidopathy. We did not include other demographic factors potentially associated with the CVI, as the smoking habitus[33] or the body mass index.[34] We mostly included patients with non-naïve DR undergoing multiple treatments, some of them with long-standing DME. The effect of some variables, such as age, type and duration of DM, or PPV, could have been missed or underestimated in our small group of naïve patients. A similar analysis in naïve DME eyes is warranted. Finally, the choroidal measurement could be biased by media opacities, signal attenuation, motion, and projection artifacts affecting the overall quality of the scans.

In conclusion, we found that diabetic choroidopathy worsens with worsening of DR, with eyes with proliferative disease having the worst reduction in choroidal vascularity. The study of the central macula region yields the most clinically relevant information. The CVI values measured on SS-OCT fairly correlate with SD-OCT, but caution is recommended in the case of extreme CVI values.

Acknowledgments

This research did not receive any specific grant from funding agencies in the public, commercial, or not-for-profit sectors.

Contributorship Statement: All the authors contributed to the conception or design of the work, the acquisition, analysis, and interpretation of data, drafting the work, revising it critically for important intellectual content. Each of the coauthors has seen and agrees with the content of this manuscript and the way their name is listed.

Disclosure: **N. Nicolini**, None; **B. Tombolini**, None; **C. Barresi**, None; **F. Pignatelli**, None; **R. Lattanzio**, None; **F. Bandello**, None; **M.V. Cicinelli**, None

References

1. Wang JC, Lains I, Providencia J, et al. Diabetic Choroidopathy: Choroidal Vascular Density and Volume in Diabetic Retinopathy With Swept-Source Optical Coherence Tomography. *Am J Ophthalmol*. 2017;184:75–83.
2. Tan KA, Laude A, Yip V, Loo E, Wong EP, Agrawal R. Choroidal vascularity index - a novel

optical coherence tomography parameter for disease monitoring in diabetes mellitus? *Acta Ophthalmol*. Nov 2016;94(7):e612–e616, doi:10.1111/aos.13044.

3. Melancia D, Vicente A, Cunha JP, Abegao Pinto L, Ferreira J. Diabetic choroidopathy: a review of the current literature. *Graefes Arch Clin Exp Ophthalmol*. 2016;254(8):1453–1461.
4. Lutty GA. Diabetic choroidopathy. *Vision Res*. 2017;139:161–167.
5. Cicinelli MV, Cavalleri M, Brambati M, Lattanzio R, Bandello F. New imaging systems in diabetic retinopathy. *Acta Diabetol*. 2019;56(9):981–994.
6. Sodhi SK, Golding J, Trimboli C, Choudhry N. Feasibility of peripheral OCT imaging using a novel integrated SLO ultra-widefield imaging swept-source OCT device. *Int Ophthalmol*. 2021;41(8):2805–2815.
7. Stanga PE, Pastor-Idoate S, Reinstein U, et al. Navigated single-capture 3D and cross-sectional wide-field OCT of the mid and peripheral retina and vitreoretinal interface. *Eur J Ophthalmol*, https://doi.org/10.1177/11206721211026100.
8. Kim MS, Lim HB, Lee WH, Kim KM, Nam KY, Kim JY. Wide-Field Swept-Source Optical Coherence Tomography Analysis of Interocular Symmetry of Choroidal Thickness in Healthy Young Individuals. *Invest Ophthalmol Vis Sci*. 2021;62(3):5.
9. Agrawal R, Ding J, Sen P, et al. Exploring choroidal angioarchitecture in health and disease using choroidal vascularity index. *Prog Retin Eye Res*. 2020;77:100829.
10. Gupta C, Tan R, Mishra C, et al. Choroidal structural analysis in eyes with diabetic retinopathy and diabetic macular edema-A novel OCT based imaging biomarker. *PLoS One*. 2018;13(12):e0207435.
11. Kim M, Ha MJ, Choi SY, Park YH. Choroidal vascularity index in type-2 diabetes analyzed by swept-source optical coherence tomography. *Sci Rep*. 2018;8(1):70.
12. Wang H, Tao Y. Choroidal structural changes correlate with severity of diabetic retinopathy in diabetes mellitus. *BMC Ophthalmol*. 2019;19(1):186.
13. Optos Silverstone; Optos PLC; Dunfermline, UK. Accessed August 7, 2021, https://www.optos.com/products/silverstone/.
14. Corvi F, Corradetti G, Parrulli S, Pace L, Staurenghi G, Sadda SR. Comparison and Repeatability of High Resolution and High Speed Scans from Spectralis Optical Coherence Tomography Angiography. *Transl Vis Sci Technol*. 2020;9(10):29.
15. Early Treatment Diabetic Retinopathy Study Research Group. Grading diabetic retinopathy from stereoscopic color fundus photographs–an extension of the modified Airlie House classification. ETDRS report number 10. *Ophthalmology*. 1991;98(5 Suppl):786–806.
16. Schneider CA, Rasband WS, Eliceiri KW. NIH Image to ImageJ: 25 years of image analysis. *Nat Methods*. 2012;9(7):671–675.
17. Agrawal R, Salman M, Tan KA, et al. Choroidal Vascularity Index (CVI)–A Novel Optical Coherence Tomography Parameter for Monitoring Patients with Panuveitis? *PLoS One*. 2016;11(1):e0146344.
18. RStudio Team. Version 1.2.5033. Updated January 1, 2020, http://www.rstudio.com/.
19. Koo TK, Li MY. A Guideline of Selecting and Reporting Intraclass Correlation Coefficients for Reliability Research. *J Chiropr Med*. 2016;15(2):155–163.
20. Zaki R, Bulgiba A, Ismail R, Ismail NA. Statistical methods used to test for agreement of medical instruments measuring continuous variables in method comparison studies: a systematic review. *PLoS One*. 2012;7(5):e37908.
21. Hidayat AA, Fine BS. Diabetic choroidopathy. Light and electron microscopic observations of seven cases. *Ophthalmology*. 1985;92(4):512–522.
22. Kakiuchi N, Terasaki H, Sonoda S, et al. Regional Differences of Choroidal Structure Determined by Wide-Field Optical Coherence Tomography. *Invest Ophthalmol Vis Sci*. 2019;60(7):2614–2622.
23. Hayreh SS. Segmental nature of the choroidal vasculature. *Br J Ophthalmol*. 1975;59(11):631–648.
24. Rizzo S, Savastano A, Finocchio L, Savastano MC, Khandelwal N, Agrawal R. Choroidal vascularity index changes after vitreomacular surgery. *Acta Ophthalmol*. 2018;96(8):e950–e955.
25. Pellegrini M, Bernabei F, Mercanti A, et al. Short-term choroidal vascular changes after aflibercept therapy for neovascular age-related macular degeneration. *Graefes Arch Clin Exp Ophthalmol*. 2021;259(4):911–918.
26. Choudhry N, Golding J, Manry MW, Rao RC. Ultra-Widefield Steering-Based Spectral-Domain Optical Coherence Tomography Imaging of the Retinal Periphery. *Ophthalmology*. 2016;123(6):1368–1374.
27. McNabb RP, Grewal DS, Mehta R, et al. Wide field of view swept-source optical coherence tomography for peripheral retinal disease. *Br J Ophthalmol*. 2016;100(10):1377–1382.
28. Uji A, Yoshimura N. Application of extended field imaging to optical coherence tomography. *Ophthalmology*. 2015;122(6):1272–1274.
29. Pichi F, Carrai P, Bonsignore F, Villani E, Ciardella AP, Nucci P. Wide-Field Spectral Domain Optical Coherence Tomography. *Retina*. 2015;35(12):2584–2592.

30. Breher K, Terry L, Bower T, Wahl S. Choroidal Biomarkers: A Repeatability and Topographical Comparison of Choroidal Thickness and Choroidal Vascularity Index in Healthy Eyes. *Transl Vis Sci Technol*. 2020;9(11):8.
31. Agrawal R, Gupta P, Tan KA, Cheung CM, Wong TY, Cheng CY. Choroidal vascularity index as a measure of vascular status of the choroid: Measurements in healthy eyes from a population-based study. *Sci Rep*. 2016;6:21090.
32. Agrawal R, Seen S, Vaishnavi S, et al. Choroidal Vascularity Index Using Swept-Source and Spectral-Domain Optical Coherence Tomography: A Comparative Study. *Ophthalmic Surg Lasers Imaging Retina*. 2019;50(2):e26–e32.
33. Kocak N, Yeter V, Subasi M, Yucel OE, Can E. Use of choroidal vascularity index for choroidal structural evaluation in smokers: an optical coherence tomography study. *Cutan Ocul Toxicol*. 2020;39(4):298–303.
34. Agarwal A, Saini A, Mahajan S, et al. Effect of weight loss on the retinochoroidal structural alterations among patients with exogenous obesity. *PLoS One*. 2020;15(7):e0235926.